Progress In Electromagnetics Research, PIER 84, 221–237, 2008

ON AVERAGING MASS OF SAR CORRELATING WITH TEMPERATURE ELEVATION DUE TO A DIPOLE ANTENNA

A. Hirata, K. Shirai, and O. Fujiwara

Department of Computer Science and Engineering
Nagoya Institute of Technology
Japan

Abstract—This study investigated the relationship between temperature elevation and spatial-average SAR (specific absorption rate) in a head model of a Japanese male due to a dipole antenna. The frequencies considered are in the range between 800 MHz and 3 GHz, which are used in wireless communications. Our attention focuses on the average mass of SAR which maximizes the correlation with local temperature elevation. Computational results suggested that an appropriate averaging mass of SAR did not exist over wide frequencies, which was attributed to the frequency-dependent penetration depth of electromagnetic waves. For most cases considered in this study the SAR averaging over 10 g was better than that for 1-g from the standpoint of correlating the temperature elevation. The dominant factor influencing this averaging mass is the thermal diffusion length which largely depends on the blood perfusion rate. Additionally, the heat evolved in the pinna played an important role in the correlation between spatial-average SAR and temperature elevation.

1. INTRODUCTION

In recent years, there has been increasing public concern about the adverse health effect due to electromagnetic (EM) waves. Therefore, public organizations over the world have been regulating safety guidelines/standards for human protection from EM wave (e.g., [1, 2]). Peak spatial-average SAR (specific absorption rate) is used as a metric for RF localized exposures. Many researchers have been investigated the human-antenna interactions with this metric [3–10]. However, physiological effects and damage to humans due to microwave energy would be induced by temperature elevation. It has been reported that

a temperature elevation 0.2 K–0.3 K in hypothalamus leads to altered thermoregulatory behavior [11]. A temperature elevation of 4.5 K in the brain has been noted to be an allowable limit, which does not lead to any physiological damage for exposures of more than 30 minutes [12]. The threshold temperature of the pricking pain in the skin is 45 K, corresponding to the temperature elevation of 10–15 K [13]. There are/were several differences of spatial-average mass and scheme for calculating peak spatial-average SAR in different guidelines/standards, although their scientific rationale should be identical.

A recent notable trend in the international guidelines/standards is that a mass for spatially averaging SAR would be harmonizing to 10 g since the averaging mass prescribed in the IEEE standard [2] has been changed from 1 g to 10 g. One of the rationales for this revision is based on the temperature elevation in the brain and eye lens, which has been computed with anatomically-based head models. For handset antennas, several groups have calculated the temperature elevation in anatomically-based human head model due to handset antennas [14–21]. Among others, we have attempted to correlate peak temperature elevations with peak spatial-average SAR [18, 21]. Then, we found that the SAR averaging mass of 10 g would be better than 1 g to correlate with local temperature elevation. This finding was explained in terms of heat diffusion length, which was roughly derived on the basis of Green's function for the bioheat equation [21]. In these studies, our attention focused on the correlation between *peak* temperature elevation and *peak* spatial-average SAR only, since the latter is a metric prescribed in the guidelines/standards. Until recently, little attention has been paid to spatial-average SAR and temperature elevation over the whole head/body. The positions of peak SAR and peak temperature elevation, however, do not always coincide with each other [18]. Also note that a position where peak spatial-average SAR appears depends on the averaging mass [22].

Bit-Babik et al. [23] investigated the effect of mass for spatial-average SAR on the correlation with temperature elevation for exposure to plane wave in the frequency between 30 MHz and 1 GHz. From the aspect of the correlation with temperature elevation, the SAR averaging mass of 5–10 g was found to be reasonable over a wide frequency band. However, the dominant factor influencing heat diffusion length is known to be the blood perfusion rate of biological tissues [21]. Additionally, the far-field source was considered in that study, although spatial-average SAR is a metric to protect humans from near-field exposures [1, 2]. Thus, it is worth re-examining the finding by Bit-Babik [23] for RF *near*-field exposure in the *head* tissue, while their investigation is informative as fundamental discussion. At

the same time, we have reported the correlation between spatial-average SAR and temperature elevation over the whole head due to a dipole antenna from 800 MHz to 3 GHz [24]. Then, we have shown that the SAR averaging mass of 10 g is better than 1 g, as is the same when considering the correlation between peak SAR and peak temperature elevation only [21].

For further clarifying the rationale of SAR averaging mass prescribed in guidelines/standards, in this study, we investigated the effect of SAR averaging mass on the correlation with temperature elevation in the head due to a dipole antenna. The SAR-temperature elevation correlation was investigated statistically for all the voxels in the whole head. The frequencies considered are in the range of 800 MHz to 3 GHz, which is used in conventional wireless communications. Note that 3 GHz is the upper frequency where peak spatial-average SAR is applicable for RF near-field exposures in the IEEE standard [2].

2. MODEL AND METHODS

2.1. Human Head Model

An anatomically-based head model developed at Nagoya Institute of Technology [25] was used in this study. This model is comprised of 17 tissues, including bone (skull), muscle, skin, fat, white matter, grey matter, cerebellum, and blood. The resolution of this model is 2 mm. The width, depth, and height of this model are 202 mm, 210 mm, and 228 mm.

2.2. FDTD Method

The FDTD (finite-difference time-domain) method [26] is used for investigating electromagnetic interaction between the human head model and a dipole antenna. The side length of the cell is 2 mm, which matches the resolution of the head model. The electrical constants of the tissues are determined with a 4-Cole-Cole extrapolation [27]. For geometries in which wave-object interaction proceeds in the open region, the computational space has to be truncated by absorbing boundaries. In this study, a 12-layered PML with a parabolic profile has been considered [26, 28]. A twelve-component approach is used to get the electric fields used for SAR calculation [29].

2.3. Source and Exposure Scenario

The frequencies considered are 800 MHz, 1.5 GHz, 2 GHz, and 3 GHz. The diameter of the dipole antenna is 1.0 mm. The length of the

antenna is 174, 90, 66, and 46 mm for 800 MHz, 1.5 GHz, 2 GHz, and 3 GHz, respectively. The feeding scheme proposed in [30] was used. The position of the antenna relative to the head model is given in Figure 1. The separation between the feeding point and the edge of right pinna is 12 mm.

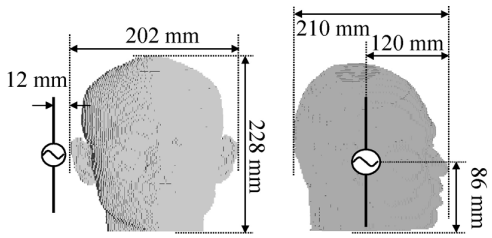

Figure 1. Relative position of realistic human head model and dipole antenna.

2.4. SAR Calculation and Basic Theory

For harmonically varying EM fields, the SAR is defined as

$$SAR = \frac{\sigma |E^2|}{\rho} \tag{1}$$

where E is the peak values of electric-field components, σ and ρ are the conductivity and mass density of the tissue. For calculating spatial-average SAR, an algorithm specified in the IEEE guidelines [30] is used. The shape of the volume is a cube, and special attention is paid to treating air and pinna.

2.5. Temperature Calculation

The temperature in the human body is calculated by solving a well-known bioheat equation [32]. The SAR calculated with the FDTD method is used as the heat source. The bioheat equation, which takes into account the heat exchange mechanisms such as heat conduction, blood perfusion, and EM heating, is represented by the following equation:

$$\begin{aligned} C(\mathbf{r})\rho(\mathbf{r})\frac{\partial T(\mathbf{r},t)}{\partial t} &= \nabla \cdot (K(\mathbf{r})\nabla T(\mathbf{r},t)) + \rho(\mathbf{r})SAR(\mathbf{r}) + Q(\mathbf{r},t) \\ &\quad -B(\mathbf{r},t)(T(\mathbf{r},t) - T_B(\mathbf{r},t)) \end{aligned} \tag{2}$$

where T is the temperature of the tissue, T_b the temperature of the blood, K the thermal conductivity of the tissue, C the specific heat of the tissue, Q the metabolic heat generation, and B the term associated with blood perfusion. Also note that $\boldsymbol{r}$ and t denotes the position vector and time.

The temperature elevation due to handset antennas can be considered as sufficiently small not to activate the thermoregulatory response; including the increase of local blood flow and the activation of sweating mechanism. The limit in the safety guidelines/standards is regulated so that temperature elevations do not exceed 1 K. Thus, this response is neglected in our study. Additionally, the blood temperature is assumed to be spatially and timely constant, since the EM power absorption due to antennas (output power of less than 1 W) is much smaller than the metabolic heat generation of adult (~ 100 W), resulting in a marginal body-core temperature elevation. Then, the Equation (2) is simplified as the following equation:

$$C(\mathbf{r})\rho(\mathbf{r})\frac{\partial T(\mathbf{r},t)}{\partial t} = \nabla\cdot(K(\mathbf{r})\nabla T(\mathbf{r},t)) + \rho(\mathbf{r})SAR(\mathbf{r}) + A(\mathbf{r}) - B(\mathbf{r})(T(\mathbf{r},t) - T_B) \tag{3}$$

Next, the boundary condition for Equation (1) is given by

$$-K(r)\frac{\partial T(\mathbf{r},t)}{\partial n} = H\cdot(T_s(\mathbf{r},t) - T_e(t)) + SW\left(\mathbf{r}, T_s(\mathbf{r},t)\right) \tag{4}$$

where H, T_s, and T_e denote, respectively, the heat transfer coefficient, the surface temperature of the tissue, and the temperature of the air. The last term SW represents the sweating effect, which we assume can be neglected in this study, since the temperature elevation due to handset is sufficiently small to activate the sweating response.

The temperature elevation in the human model due to EM waves gets saturated or becomes maximal at the thermally steady state. For this reason, the temperature elevation at the thermally steady state is considered in this paper, corresponding to the worst-case evaluation. Equations (3) and (4) are reduced to the following equations at the thermally steady state:

$$C(\mathbf{r})\rho(\mathbf{r})\frac{\partial \delta T(\mathbf{r},t)}{\partial t} = \nabla\cdot(K(\mathbf{r})\nabla\delta T(\mathbf{r},t)) + \rho(\mathbf{r})SAR(\mathbf{r}) - B(\mathbf{r},t)\delta T(\mathbf{r},t) \tag{5}$$

$$\left(H + K(\boldsymbol{r})\frac{\partial}{\partial n}\right)\delta T(\boldsymbol{r}) = 0 \tag{6}$$

where $\delta T(\boldsymbol{r})$ is the temperature elevation of tissue. Equation (5) is a linear differential equation subject to the boundary condition (6).

The Equation (3) with the boundary condition (4) means that the temperature elevation and SAR distributions do not correspond to each other. However, from Equations (5) and (6), the temperature elevation at the thermally steady state is linear in terms of the output power of the antenna, or the SAR amplitude. Note that it takes 30 minutes or more till the temperature elevation gets saturated. It is also noteworthy that Q and C do not influence the temperature elevation at the thermally steady state from these equations.

From equations of (5) and (6), the steady-state temperature elevation is given by the following equation [21]:

$$\delta T(\mathbf{r}) = \sum_i \rho(\mathbf{r}_i) SAR(\mathbf{r}_i) G(\mathbf{r}; \mathbf{r}_i) \tag{7}$$

where G is Green's function. In biological tissues, the dominant parameter influencing this function is revealed to be the blood perfusion rate. A detailed discussion on this function is given in our previous study [21]. Equation (7) suggests that the temperature elevation would be mainly governed by the SAR distribution and blood perfusion rate of tissues.

The thermal parameters used in this study are given in Table 1, which is the same as in [18]. They are borrowed from [16, 33]. The heat transfer coefficient between the model surface and air was set to $5\,\mathrm{Wm^{-2}\,K^{-1}}$, which is the typical value at the room temperature of 23°C [34]. Samaras et al. [35] pointed out the weakness of boundary condition for the bioheat equation when applied to the human model with the stair-casing approximation. Recently, an improved algorithm for reducing computational error has been proposed by Neufeld et al. [36]. Such an algorithm would be essential when calculating the temperature itself. However, that error does not influence temperature *elevation* so much as shown in Wang and Fujiwara [13], e.g., due to the linearity of bioheat equation at the thermally steady state. Thus we used the conventional formula given in this section. Note that the difference in the heat transfer coefficients reported in previous studies is comparable to or larger than the above-mentioned uncertainty (summarized in [34]).

3. COMPUTATIONAL RESULTS AND DISCUSSION

We calculated the temperature elevation and spatial-average SAR in the head model. The frequencies considered are 800 MHz and 3 GHz in this discussion. The spatial-average SAR was calculated on the basis of the IEEE standard [2]. We considered the relationship between spatial-average SAR and temperature elevation at the datum point

Table 1. Thermal constants of tissues.

Tissue	K [W K m^{-1}]	C [J K kg^{-1}]	B [W K m^{-3}]	ρ [kg m^{-3}]	A [W m^{-3}]
Internal air	0.03	1000	0	1.2	0
Skin	0.42	3600	9100	1125	1620
Muscle	0.5	3800	2700	1047	480
Fat	0.25	3000	1700	916	300
Cartilage	0.47	3600	9000	1097	1600
Bone Marrow	0.22	3000	32000	1040	5700
Gray Matter	0.57	3800	40000	1038	7100
White Matter	0.5	3500	40000	1038	7100
CSF	0.62	4000	0	1007.2	0
Vitreous Humor	0.58	4000	0	1008.9	0
Cornea	0.52	3600	0	1076	0
Lens	0.4	3000	0	1053	0
Sclera	0.58	3800	75000	1026	22000
Blood	0.56	3900	0	1058	0
Glands	0.53	3500	360000	1050	64000
Mucous Membrane	0.5	3600	9000	1040	1600
Dura	0.5	3600	9100	1125	0
Skull	0.39	3100	3300	1850	610

of average SAR. We chose two averaging masses as 1 g and 10 g. Note that the mass of 1 g corresponds to the value prescribed in the previous IEEE standard [37], and 10 g to that in the ICNIRP guidelines [1] and the revised IEEE standard [2]. Since we choose the shape of the averaging volume as a cube, its side length is approximately 2 mm, 10 mm, and 22 mm, respectively, assuming that the mass density is uniform at 1000 kg m^{-3}. Note that the side length of averaging volume in the actual situation is somewhat different from the above values due to the heterogeneity of tissue (or different mass density), the curvature of the model, and a unique averaging algorithm prescribed in the IEEE standard [31]. The ratio of $\Delta T/SAR_{avg}$ is called the heating factor in the following discussion.

Figure 2 illustrates the heating factor for (a) voxel SAR and SAR averaged over (b) 1 g and (c) 10 g on the horizontal cross section across the ear canal. As seen from Figure 2, the larger the SAR averaging mass is, the smoother the heating factor distribution is. Note that

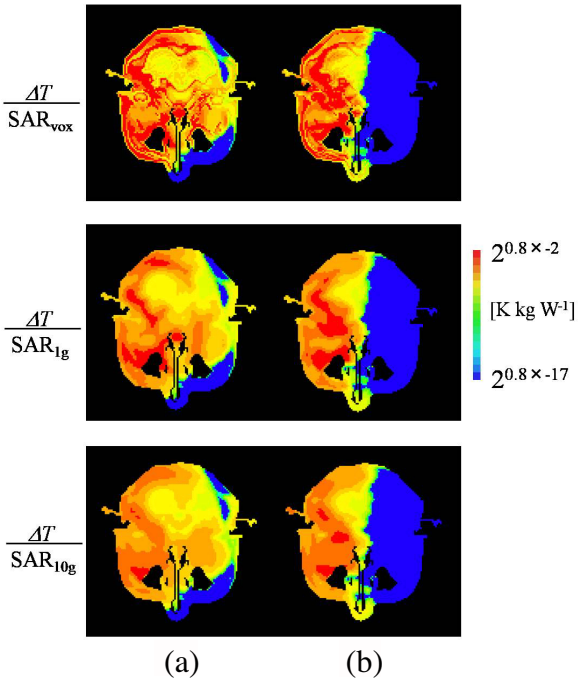

Figure 2. Heating factors for (a) voxel, (b) 1-g and (c) 10-g average SARs on the horizontal cross section of a head model across the ear canal.

the heating factor distribution is determined by the balance of average SAR and temperature elevation distributions. The SAR distribution is known to be not so smooth due to different conductivity in different tissues (e.g., [38, 39]). This is mainly attributed to the difference of water content: the higher the water content of tissue, the higher the conductivity of tissue becomes [34]. The SAR averaging over specific mass, on the other hand, is known to be smooth [40]. The temperature elevation distribution due to microwave energy is rather smooth due to heat diffusion (e.g., [13, 18]). Thus, an appropriate mass for averaging SAR would not be estimated in a straightforward manner.

From the same figure, a higher heating factor is observed not at the surface of the head but in the interior part of the head. Tissues at corresponding parts are mainly the bone or fat. The conductivity of these tissues is small, resulting in small SAR (see Equation (1)). In addition to this, temperature elevation becomes relatively large due to the heat diffused from the head surface and/or the pinna where EM

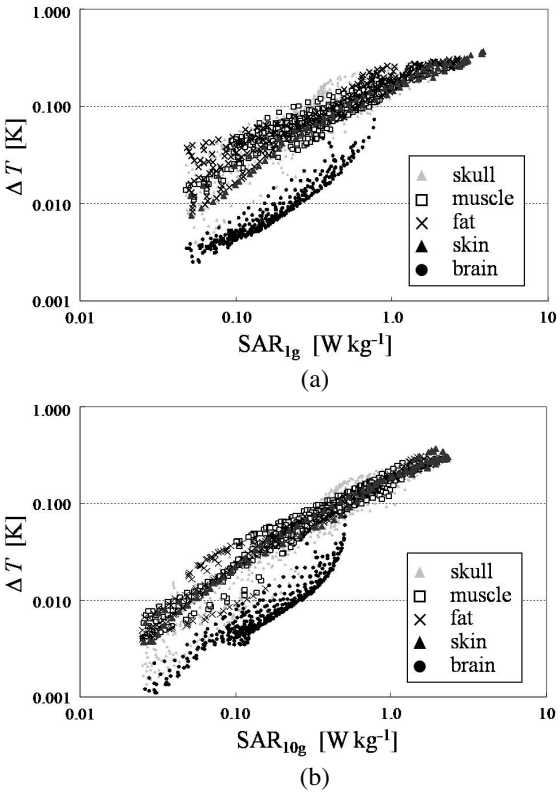

Figure 3. Temperature elevation versus SAR averaged over (a) 1 g and (b) 10 g tissues for voxels on a horizontal cross section of the head model across the ear canal.

power absorption is concentrated. A lower heating factor is observed in the brain than in the other part. The main reason for this would be its large blood perfusion rate, as suggested in [21] and [24]. In order to definitely confirm this, 1-g and 10-g average SARs versus temperature elevation are plotted in Figure 3 on a logarithmic scale. The frequency is 800 MHz. Note that we have plotted for voxels whose average SAR is larger than the corresponding peak value multiplied by one hundredth. This is because computational accuracy may not be reliable for a small SAR value. Additionally, small temperature elevation is not essential for human protection against EM wave exposure. As seen from Figure 3, a significant difference in the plots between the brain and other tissues was found for the averaging mass of 1 g. A similar tendency was also observed for the average mass

of 10 g, but the plots are relatively converged. Note that the heat capacity and heat conductivity of tissues do not influence temperature elevation [18]. Thus, it is suggested that the blood perfusion rate is one of the dominant factors influencing the correlation with average SAR and temperature elevation. Except for the brain plots, a reasonable correlation is found between spatial-average SARs and temperature elevation for the other tissues.

Based on the above fundamental characteristics, the effect of averaging mass on the correlation of spatial-average SAR and temperature elevation was evaluated by the method of least square, assuming that the relation between temperature elevation and spatial-average SAR is linear. The rationale for this assumption is that Maxwell's equation and steady-state bioheat equation are linear. The intercept is chosen as nonexistent as no temperature elevates without EM exposure. The coefficient of determination was used as a measure to evaluate the correlation. The less the calculated values depart from the regression line, the closer to unity the coefficient of determination is. Note that the SAR in the center of the head and the other side from the antenna is extremely small and does not reach acceptable computational accuracy due to the frequency-dependent penetration depth of EM waves. For this reason, we define two thresholds as compared with peak voxel SAR in the head excluding the pinna: i) one hundredth and ii) $1/e$ or EM penetration depth.

Figures 4 and 5 illustrate the influence of averaging mass on the correlation for the cases i) and ii), respectively. As seen from Figure 4(a), the coefficient of determination took a maximum in the range of 15–30 g for the frequency below 2 GHz. On the other hand, the appropriate average mass at 3 GHz decreases to 8 g at 3 GHz. This difference was explained in terms of Equation (7). The temperature elevation at a specific position is mainly determined by the SAR and blood perfusion rate around there. As presented in [20], the heat evolved diffuses up to a few centimeters or more. Assuming that the averaging shape is a cube, the side length of averaging volume should be larger than a few centimeters at least. However, due to the concentration of SAR distribution at higher frequencies, an appropriate averaging mass would decrease with the increase of the frequency of EM waves. From Figure 4(b), the heating factor becomes large with the increase of SAR averaging mass. The region in which EM energy is not much penetrated is included for large average volume, resulting in a larger heating factor. The heating factor also depends on the frequency. Different EM frequencies result in different SAR distribution or penetration depth. Now we consider the correlation between spatial-average SAR and temperature elevation for voxels

whose SAR is larger than one hundredth of the peak value. The number of each tissue included for consideration is different for different frequencies of EM waves. The energy deposited in the pinna is also influenced by the frequency of EM waves.

Comparing Figures 4(a) and 5(a), a different tendency was observed. The coefficient of determination for case (ii) is smaller than that for case (i). In case (ii), main peak appears at around 50 g for frequencies below 3 GHz, or shifted to larger averaging mass as

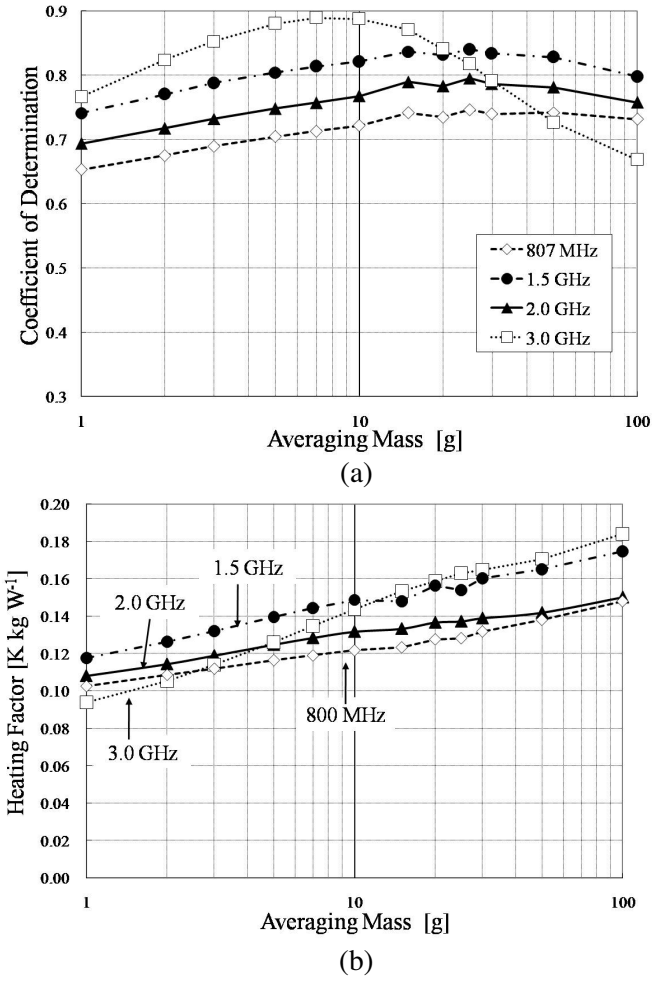

Figure 4. Effect of average mass on (a) heating factor and (b) coefficient of determination for case (i).

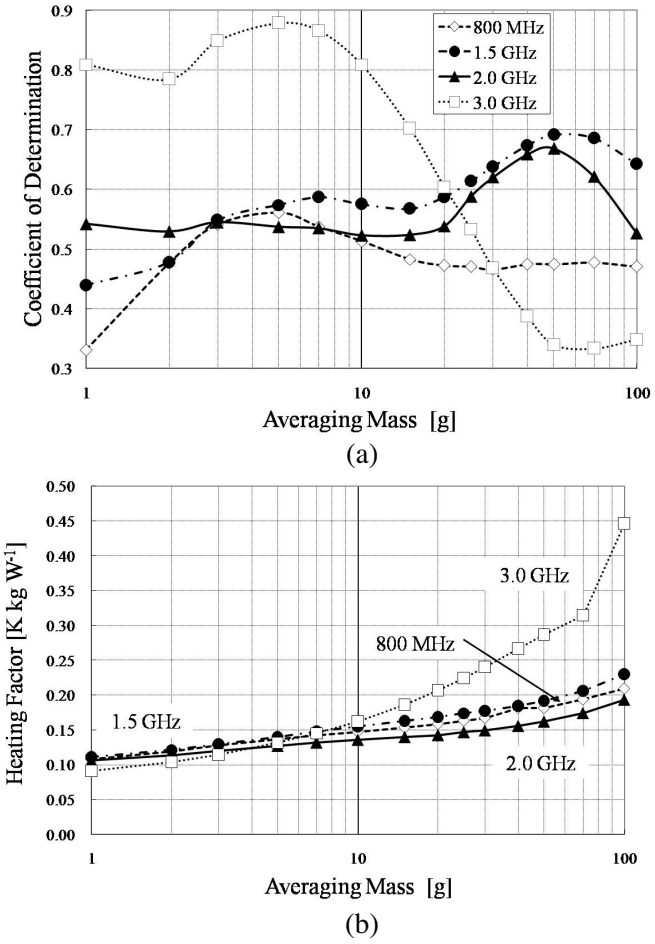

Figure 5. Effect of average mass on (a) heating factor and (b) coefficient of determination for case (ii).

compared to case (i). We observe that this difference was caused by the EM energy deposited in the pinna due for the following reason. When the antenna is located in close proximity to the head, much energy is deposited around the pinna. Note that the pinna is not included in the SAR averaging procedures in the IEEE standard [31]. The heat evolved in the human tissues can diffuse up to a few centimeters. Thus, the EM energy in the pinna affects the temperature elevation in the remaining part of the head. From Figures 4(b) and 5(b), the heating factors for case (ii) are larger than those for case (i). In case (ii),

the region considered is limited to that around the pinna due to the precondition. Then, the effect of heat diffused from the pinna would be larger than that for case (i). From this figure, somewhat different results would be expected for other body parts, due to different blood perfusion rate and curvature of body model. This is the main reason for the difference of average mass between our results and Bit-Babik et al. [23].

4. SUMMARY AND CONCLUDING REMARKS

This study investigated the relationship between temperature elevation and spatial-average SAR (specific absorption rate) in a head model of a Japanese male due to a dipole antenna in the frequency from 800 MHz to 3 GHz. 3 GHz is the upper frequency where peak spatial-average SAR is applicable for RF near-field exposures in the IEEE standard [2]. Our attention focused on the average mass of SAR which maximizes the correlation with local temperature elevation over the head. The rationale for this investigation was that temperature elevation was the dominant factor inducing physiological response due to EM energy. Thus, the spatial-average SAR, which is a metric for human protection, should correlate with temperature elevation.

Computational results did not suggest that an appropriate average mass of SAR exist over wide frequencies. The main reason for this was that the effect of blood perfusion rate of tissues on the correlation was significant. Added to this, the SAR distribution depended on the frequency. However, for the cases considered in this study, 10-g SAR was better than 1-g for correlating the temperature elevation. This is attributed to the heat diffusion length, as can be seen from our previous study [21]. For other body parts, somewhat different results would be expected due to different blood perfusion rate and curvature of body model. This is the main reason for the difference between our results and Bit-Babik et al. [23].

In a future work, we will increase the frequency of EM waves to 10 GHz, which is the upper frequency of spatial-average SAR prescribed in the ICNIRP guidelines [1].

ACKNOWLEDGMENT

This work was partially supported by the Ministry of Education, Science, Sports, and Culture, Grant-in-Aid for young scientist (B), the Hori information science promotion foundation and the Foundation of Ando Laboratory, Japan.

REFERENCES

1. ICNIRP, "Guidelines for limiting exposure to time-varying electric, magnetic and electromagnetic fields (up to 300 GHz)," *Health Phys.*, Vol. 74, 494–522, 1998.
2. IEEE, C95.1 IEEE standard for safety levels with respect to human exposure to radio frequency electromagnetic fields, 3 KHz to 300 GHz, IEEE, New York, 2005.
3. Kang, X. K., L. W. Li, M. S. Leong, and P. S. Kooi, "A method of moments study of SAR inside spheroidal human head and current distribution along handset wire antennas," *J. Electromagnetic Waves and Appl.*, Vol. 15, No. 1, No. 61–75, 2001.
4. Kouveliotis, N. K., P. J. Papakanellos, E. D. Nanou, N. I. Sakka, V. S. G. Tsiafkis, and C. N. Capsalis, "Correlation between SAR, SWR and distance of mobile terminal antenna in front of a human phantom: Theoretical and experimental validation," *J. Electromagnetic Waves and Appl.*, Vol. 17, No. 11, No. 1561–1581, 2003.
5. Pino, A. G., M. Arias, M. G. Sanchez, I. Cuinas, and A. A. Alonso, "Determination of safety volumes for medium-frequency emissions under standard limits of human exposure," *J. Electromagnetic Waves and Appl.*, Vol. 17, No. 11, 1605–1611, 2003.
6. Yoshida, K., A. Hirata, Z. Kawasaki, and T. Shiozawa, "Human head modeling for handset antenna design at 5 GHz band," *J. Electromagnetic Waves and Appl.*, Vol. 19, No. 3, 401–411, 2005.
7. Kiminami, K., A. Hirata, Y. Horii, and T. Shiozawa, "A study on human body modeling for the mobile antenna design at 400 MHz band," *J. Electromagnetic Waves and Appl.*, Vol. 19, No. 5, 671–687, 2005.
8. Kuo, L. C., Y. C. Kan, and H. R. Chuang, "Analysis of a 900/1800-MHz dual-band gap loop antenna on a handset with proximate head and hand model," *J. Electromagnetic Waves and Appl.*, Vol. 21, No. 1, 107–122, 2007.
9. Ebrahimi-Ganjeh, M. A. and A. R. Attari, "Interaction of dual band helical and PIFA handset antennas with human head and hand," *Progress In Electromagnetics Research*, PIER 77, 225–242, 2007.
10. Liu, Y., Z. Liang, and Z. Q. Yang, "Computation of electromagnetic dosimetry for human body using parallel FDTD algorithm combined with interpolation technique," *Progress In Electromagnetics Research*, PIER 82, 95–107, 2008.
11. Adair, E. R., B. W. Adams, and G. M. Akel, "Minimal changes

in hypothalamic temperature accompanymicrowave-induced alteration of thermoregulatory behavior," *Bioelectromagnetics*, Vol. 5, 13–30, 1984.

12. Guyton, A. C. and J. E. Hall, *Textbook of Medical Physiology*, W. B. Saunders, Philadelphia, PA, 1996.
13. Hardy, J. D., H. G. Wolff, and Goodell, *Pain Sensation and Reactions*, Chap. IV and X, Williams & Wilkis, Baltimore, MD, 1952.
14. Wang, J. and O. Fujiwara, "FDTD computation of temperature rise in the human head for portable telephones," *IEEE Trans. Microwave Theory & Tech.*, Vol. 47, 1528–1534, 1999.
15. Van Leeuwen, G. M. J., J. J. W. Lagendijk, B. J. A. M. Van Leersum, A. P. M. Zwamborn, S. N. Hornsleth, and A. N. T. Kotte, "Calculation of change in brain temperatures due to exposure to a mobile phone," *Phys. Med. Biol.*, Vol. 44, 2367–2379, 1999.
16. Bernardi, P., M. Cavagnaro, S. Pisa, and E. Piuzzi, "Specific absorption rate and temperature increases in the head of a cellularphone user," *IEEE Trans. Microwave Theory & Tech.*, Vol. 48, 1118–1126, 2000.
17. Wainwright, P., "Thermal effects of radiation from cellular telephones," *Phys. Med. Biol.*, Vol. 45, 2363–2372, 2000.
18. Hirata, A. and T. Shiozawa, "Correlation ofmaximum temperature increase and peak SAR in the human head due to handset antennas," *IEEE Trans. Microw. Theory Tech.*, Vol. 51, No. 7, 1834–1841, July 2003.
19. Hirata, A., M. Morita, and T. Shiozawa, "Temperature increase in the human head for dipole antenna at microwave frequencies," *IEEE Trans. Electromagnetic Compat.*, Vol. 45, No. 1, 109–116, 2003.
20. Ibrahiem, A., C. Dale, W. Tabbara, and J. Wiart, "Analysis of the temperature increase linked to the power induced by RF source," *Progress In Electromagnetics Research*, PIER 52, 23–46, 2005.
21. Hirata, A., M. Fujimoto, T. Asano, J. Wang, O. Fujiwara, and T. Shiozawa, "Correlation between maximum temperature increase and peak SAR with different average schemes and masses," *IEEE Trans. Electromagnetic Compat.*, Vol. 48, 569–578, 2006.
22. Burkhart, M. and N. Kuster, "Appropriate modeling of the ear for compliance testing of handheld MTE with SAR safety limits at 900/1800 MHz," *IEEE Trans. Microwave Theory Tech.*, Vol. 48, 1927–1934, 2000.

23. Bit-Babik, G., A. Faraone, C. K. Chou, A. Radmadze, and R. Zaridze, "Correlation between locally averaged SAR distribution and related temperature rise in human body exposed to RF field," *Proc. BEMS 2007*, 2–5, 2007.
24. Hirata, A., K. Shirai, and O. Fujiwara, "Relationship between temperature elevation and spatial average SAR in Japanese human head model due to dipole antenna," *IEEE International Symposium on Electromagnetic Compatibility*, WE-PM-2-SS-7, 2007.
25. Wang, J. and O. Fujiwara, "Dosimetric evaluation of human head for portable telephones," *Electron. Commun. Japan*, Part I, Vol. 85, No. 7, 12–22, July 2002.
26. Taflove, A. and S. Hagness, *Computational Electrodynamics: The Finite-Difference Time-Domain Method*, 2nd edition, Artech House, Norwood, MA, 2003.
27. Gabriel, C., "Compilation of the dielectric properties of body tissues at RF and microwave frequencies," Final Tech. Rep. Occupational and Environmental Health Directorate, AL/OE-TR-1996-0037 (Brooks Air Force Base, TX: RFR Division), 1996.
28. Volakis, J. L., K. Caputa, M. Okoniewski, and M. A. Stuchly, "An algorithm for computations of the power deposition in human tissue," *IEEE Antenna Propagat. Mag.*, Vol. 41, No. 4, 102–107, 1999.
29. Yu, W., D. H. Werner, and R. Mittra, "Finite Difference Time Domain (FDTD) analysis of an artificially-synthesized absorbing medium," *J. Electromagnetic Waves and Appl.*, Vol. 15, No. 8, 1005–1026, 2001.
30. Watanabe, S. and M. Taki, "An improved FDTD model for the feeding gap of a thin-wire antenna," *IEEE Microwave & Guided Wave Letts.*, Vol. 8, 152–154, 1999.
31. IEEE C95.3, IEEE Recommended Practice for Measurements and Computations of Radio Frequency, IEEE, New York, 2002.
32. Pennes, H. H., "Analysis of tissue and arterial blood temperature in resting forearm," *J. Appl. Physiol.*, Vol. 1, 93–122, 1948.
33. Duck, F. A., *Physical Properties of Tissue*, Academic, New York, 1990.
34. Fiala, D., K. J. Lomas, and M. Stohrer, "A computer model of human thermoregulation for a wide range of environmental conditions: The passive system," *J. Appl Physiol.*, Vol. 87, 1957–1972, 1999.
35. Samaras, T., A. Christ, and N. Kuster, "Effects of geometry

discretization aspects on the numerical solution on the bioheat transfer equation with the FDTD technique," *Phys. Med. Biol.*, Vol. 51, N221–N229, 2006.

36. Neufeld, E., N. Chavannes, T. Samaras, and N. Kuster, "Novel conformal technique to reduce staircasing artifacts at material boundaries for FDTD modeling of the bioheat equation," *Phys. Med. Biol.*, Vol. 52, 4371–4381, 2007.
37. IEEE C95.1, IEEE Standard for Safety Levels with Respect to Human Exposure to Radio Frequency Electromagnetic Fields, 3 KHz to 300 GHz, IEEE, New York, 1991.
38. Gandhi, O. P., G. Lazzi, and C. M. Furse, "Electromagnetic absorption in the human head and neck for mobile telephones at 835 and 1900 MHz," *IEEE Trans. Microwave Theory and Tech.*, Vol. 44, No. 10, 1884–1897, 1996.
39. Watanabe, S., M. Taki, T. Nojima, and O. Fujiwara, "Characteristics of the SAR distributions in a head exposed to electromagnetic fields radiated by a hand-held portable radio," *IEEE Trans. Microwave Theory and Tech.*, Vol. 44, No. 10, 1874–1883, 1996.
40. Okoniewski, M. and M. A. Stuchly, "A study of the handset antenna and human body interaction," *IEEE Trans. Microwave Theory & Tech.*, Vol. 44, 1855–1864, 1996.